

Boundary effects and superconducting boundary states in multi-band systems

Andrea Benfenati,^{1,*} Albert Samoilenka,¹ and Egor Babaev¹

¹*Department of Theoretical Physics, The Royal Institute of Technology, Stockholm SE-10691, Sweden*

(Dated: November 24, 2020)

We present a microscopic study of the behavior of the order parameters near boundaries of a two-band superconducting material, described by the standard tight-binding Bardeen-Cooper-Schrieffer model. We find that the relative difference between bulk and surface critical temperatures is a nontrivial function of the interband coupling strength. In general the boundary induces a nontrivial gradient of the gap ratio in different bands. For superconductors with weak interband coupling, the gap ratios near the edges and in the corners of the sample can be substantially different than in the bulk.

INTRODUCTION

The majority of the superconductors of current interest have multiple superconducting bands [1, 2] with a widely varying strength of the interband coupling. The gaps can be characterized by variety of probes, some of which selectively probe surfaces, while others are dominated by the bulk response [3–10]. The series of experimental works [11–13] reported that, on the surface of ZrB₁₂, the characteristics of the superconducting gaps are widely different compared to the bulk. According to [12, 14, 15] ZrB₁₂ is a multiband superconductor with weak interband coupling. A partial summary of the experimentally observed discrepancies concerning surface/bulk gap structure can be found in Table I in [12]. The surface effects are quite strong compared to other reported experimental examples of enhanced surface superconductivity [16–22]. An explanation for the gaps behavior in ZrB₁₂ proposes a different phonon-electron interaction on the surface of the material [23]. However, the recent works [24, 25] report that enhanced superconductivity near the boundary is a generic property of the standard single-band Bardeen-Cooper-Schrieffer model.

That raises the question of the nature of surface states in a generic multi-band Bardeen-Cooper-Schrieffer model [1, 2]. This question is addressed in the present paper. In this work we focus on clean surfaces that, as we will see below, produce pairing enhancement. We do not consider the effects of surface-induced interband single-particle scattering [26].

We consider a Fermi-Hubbard Hamiltonian describing a two-band *s*-wave superconductor. For a *d* dimensional hypercubic lattice it reads

$$H = \sum_{i,j,\sigma,\alpha} \psi_{i\sigma\alpha}^\dagger h_{ij\sigma\alpha} \psi_{j\sigma\alpha} - \sum_{i\alpha,\beta} V_{\alpha\beta} \psi_{i\uparrow\alpha}^\dagger \psi_{i\downarrow\alpha}^\dagger \psi_{i\downarrow\beta} \psi_{i\uparrow\beta}. \quad (1)$$

The roman indices *i, j* label the position on a lattice with *N* lattice points. $\sigma = \uparrow, \downarrow$ indicates the spin, while $\alpha, \beta = 1, 2$ label the component. Then $h_{ij\sigma\alpha} = -\mu\delta_{ij} - t\delta_{|i-j|,1}$, where $|i-j| = 1$ if *i* and *j* are neighboring points in

hypercubic lattice. μ is the chemical potential and *t* the hopping coefficient. In order to ensure the Hamiltonian to be hermitian, we have $h_{ij\sigma\alpha} = h_{ji\sigma\alpha}^*$ and $V_{\alpha\beta} = V_{\beta\alpha}^*$. Then, following the steps in [27], we make the mean field approximation. Introducing the Nambu spinors

$$\Psi_\alpha^\dagger = \left(\psi_{1\uparrow\alpha}^\dagger, \dots, \psi_{N\uparrow\alpha}^\dagger, \psi_{1\uparrow\alpha}, \dots, \psi_{N\uparrow\alpha} \right) \quad (2)$$

$$\Psi_\alpha = \left(\psi_{1\uparrow\alpha}, \dots, \psi_{N\uparrow\alpha}, \dots, \psi_{1\uparrow\alpha}^\dagger, \dots, \psi_{N\uparrow\alpha}^\dagger \right)^T,$$

the total mean field Hamiltonian reads

$$H_{MF} = \sum_{\alpha=1}^2 \Psi_\alpha^\dagger H_\alpha \Psi_\alpha. \quad (3)$$

H_α is the α -band Hamiltonian, defined as

$$H_\alpha = \begin{pmatrix} h_{\uparrow\alpha} & \Delta_\alpha \\ \Delta_\alpha^\dagger & -h_{\downarrow\alpha}^T \end{pmatrix}, \quad (4)$$

where the elements $h_{ij\sigma\alpha}$ have been defined above. Finally, the self-consistency equations for the gaps are:

$$\Delta_{i\alpha} = \sum_{\beta=1}^2 V_{\alpha\beta} \langle c_{i\uparrow\beta} c_{i\downarrow\beta} \rangle_\beta. \quad (5)$$

The thermal average $\langle \cdot \rangle_\beta$ means it is performed over the eigenvalues of the hamiltonian H_β . We can rewrite the self consistency equation by introducing the auxiliary vectors $(\mathbf{e}_i)_j = \delta_{i,j}$ and $(\mathbf{h}_i)_j = \delta_{j,i+N}$ as

$$\Delta_{i\alpha} = \sum_{\beta=1}^2 V_{\alpha\beta} \mathbf{e}_i f(H_\beta) \mathbf{h}_i, \quad (6)$$

with $f(x) = (1 + e^{x/T})^{-1}$ being the Fermi-Dirac function. We solve self-consistently for the gaps $\Delta_{i\alpha}$, using Chebyshev polynomial expansion method [28–30], with polynomial up to order 1000. The convergence criterion we adopt is $|\Delta_{i\alpha}^{(n+1)} - \Delta_{i\alpha}^{(n)}|/|\Delta_{i\alpha}^{(n)}| \leq 10^{-8}$, where *n* numbers the iteration. We consider both a 1D lattice with $N = 1000$ sites and a 2D square lattice with $N_x N_y = 60 \times 60$. The solver is a custom CUDA implementation. To calculate the critical temperatures, we solve the linearized version of the self consistency equation (6). For details, see [24].

RESULTS

Effects of interband coupling

We begin by analyzing a 2-band system with weak interband coupling and similar intraband interaction in two bands. The model is rescaled so that all the quantities are given in units of the hopping coefficient t . We fix $\mu = 0$, i.e. half filled bands, $V_{11} = 1.35$ and $V_{22} = 1.36$. We compare the results for non-zero interband interaction V_{12} with the case where the bands are decoupled, i.e. $V_{12} = 0.0$. In the latter, the problem is reduced to two copies of the model studied in [24] and shown to have two different critical temperatures, one for bulk states and one for boundary states. We denote by T_{c1} the bulk critical temperature, i.e. when the order parameter vanishes in the bulk. T_{c2} is the boundary critical temperature, i.e. when the order parameter vanishes on the boundaries of the superconductor. When $V_{12} = 0$ the critical temperatures in the system are: $T_{c1}^{\text{band1}} = 0.0429$ and $T_{c2}^{\text{band1}} = 0.0536$ for band 1, $T_{c1}^{\text{band2}} = 0.045$ and $T_{c2}^{\text{band2}} = 0.0562$ for band 2. Hence, the second band has a critical temperatures 5% higher than the first. Figure 1 shows the numerically obtained gaps Δ_1 and Δ_2 , displayed at various temperatures and interband coupling. In accordance with the results obtained by different analytical and numerical methods in [24], when $V_{12} = 0$, the boundary-enhancement of each gap decays to the bulk value with independent coherence length. As the coupling is turned on, $U(1)$ is broken, since the carriers in the individual bands are no longer independently conserved and there are no independent transitions for different bands.

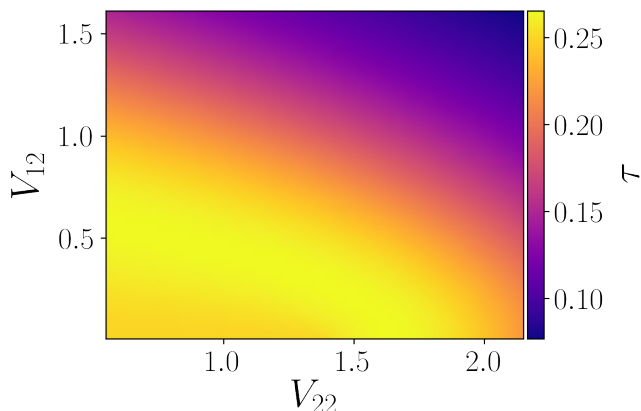


FIG. 2. Relative increase of the boundary critical temperature with respect to the bulk critical temperature as a function of the pairing potential of the second band V_{22} and of the interband coupling V_{12} . We define $\tau = (T_{c2} - T_{c1})/T_{c1}$. For a given value of V_{22} , τ exhibit a non monotonic behavior as a function of interband coupling V_{12} . $V_{11} = 1.35$ and $\mu = 0$.

Then, for non-zero V_{12} , the bulk critical temperatures

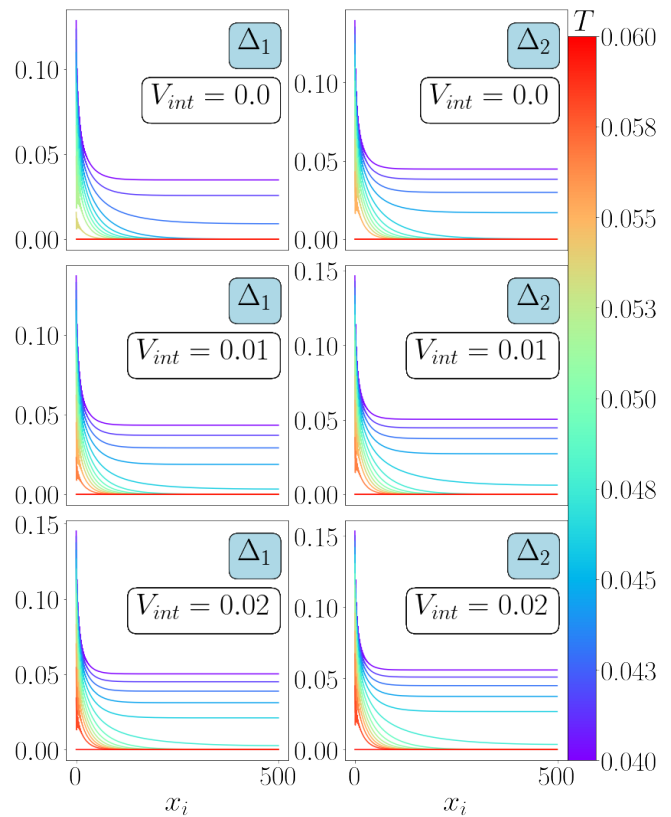


FIG. 1. Numerical solution for the two gaps at different values of the interband coupling. The boundary is located at $x = 0$. For $V_{int} = 0.0$, the two bands have different boundary and bulk critical temperatures. When the interband interaction is on, the two bands present the same critical temperatures. Yet, the weak interband coupling does not drastically affect the structure of the solution. The gaps exhibit different enhancement near the boundary and the overall solution shows the presence of different length scales. For $V_{12} = 0.01$ we have $T_{c1} = 0.0458$ and $T_{c2} = 0.0573$. For $V_{12} = 0.02$ the critical temperatures increase respectively to $T_{c1} = 0.0472$, $T_{c2} = 0.0591$. Here we show only the left half of the system.

become the same for both bands. Also the surface critical temperature is only one. The gaps behaviour near the boundaries is nontrivial as it includes relative variations of the gap values. In the case displayed in Figure 1 we have $T_{c1} = 0.0458$ and $T_{c2} = 0.0573$ for $V_{12} = 0.01$; $T_{c1} = 0.0472$ and $T_{c2} = 0.0591$ for $V_{12} = 0.02$.

We conclude this section by moving beyond the weak coupling limit and investigate the relative increase of the boundary critical temperature T_{c2} , with respect to the bulk temperature T_{c1} , as a function of inter-band coupling V_{12} . To efficiently measure this increase, we define $\tau = (T_{c2} - T_{c1})/T_{c1}$. The numerical solutions for a one dimensional model are shown on the Figure 2 for various values of V_{22} . We find that the dependence is non-trivial: at relatively weak interband coupling, τ first increases with V_{12} and then, it starts to decrease.

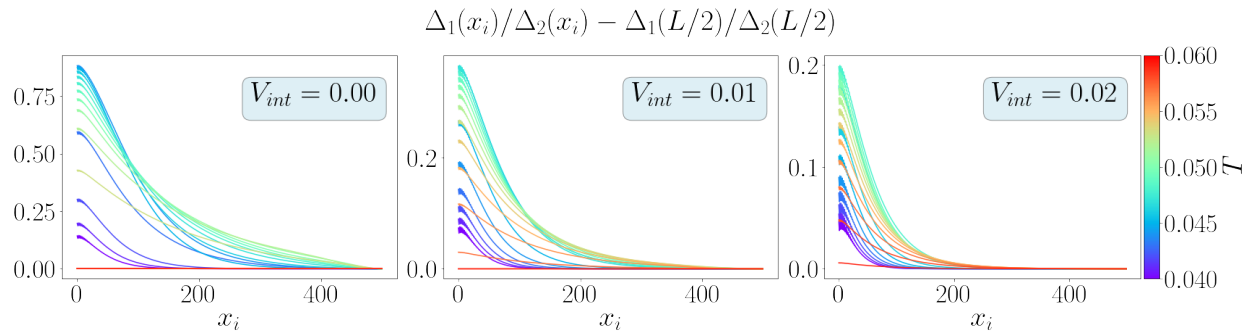


FIG. 3. Plot of gap ratios shifted by the bulk value. We can notice that the gaps ratio near the surface is evidently enhanced compared to the bulk value. The presence of weak inter-band coupling does not qualitatively change this effect. Moreover, the length scale of the penetration into the bulk shows a non monotonic behaviour as a function of T , as more accurately displayed in Figure 4. We show only half of the system (500 out of $L = 1000$ sites), since the second half is entirely symmetrical. The parameters used for this simulations are $V_{11} = 1.35$, $V_{22} = 1.36$ and $\mu = 0$.

The relative behavior of the gaps in two-band systems: boundaries vs bulk

An important characteristic of a multiband superconductor is the ratio of the gaps of different bands. Figure 3 shows the gaps ratio shifted by its bulk values at various temperatures T and inter-band coupling V_{12} for a 1D system as a function of distance from the boundary. The system we consider first has the intraband potential of the second band only 1% bigger than the first one, namely $V_{11} = 1.35$ and $V_{22} = 1.36$.

Even for these similar gap characteristics, we find that the gaps ratio can be different on the boundary of a superconductor compared to its bulk value, when the inter-band coupling is weak. Figure 3 displays the results for $V_{12} = 0.01, 0.02$ and compares them to the decoupled-bands case. In particular, we notice that the gaps ratio is enhanced near the ends of the sample, and this enhancement decays into the interior of the superconductor on a macroscopic length scale. Importantly, the surface gaps ratio deviation has not only a strong temperature dependence in magnitude, but also its length scale varies as a function of T . We can study the latter's behavior in further details by fitting the tails (i.e. after $N=50$ sites from the boundary) of the gaps ratio deviations reported in Figure 3, with an exponential function $f(x) \propto e^{-x/\xi}$. $\xi(T)$ measures the length scale of the decay into the bulk. The result, reported in Figure 4 confirms the non-monotonic behavior of $\xi(T)$ as a function of T .

The long range character associated with the relative variations of the gaps, and its non-monotonicity is consistent with the conclusions obtained for the vortex core solutions in weakly interacting two-band systems in [31–33]. At higher values of the inter-band coupling, we can notice that the relative variation of the gaps profile near the surfaces decreases, both in amplitude and

in its spatial extension, as Figure 5 reports. This remains consistent with the hybridization of bulk coherence lengths and their dependence on interband coupling strength [31]. When the interband coupling V_{12} becomes of the same order of magnitude as the intraband coupling V_{11} and V_{22} , e.g. $V_{12} = 1.0$, the enhancement of the gaps ratio basically disappears. Note that the disappearance of this variation is similar to the condition for the disappearance of the second coherence lengths in the clean two-band BCS semi-classical model found in [31]. This confirms that the width of the boundary states is determined by the bulk coherence lengths.

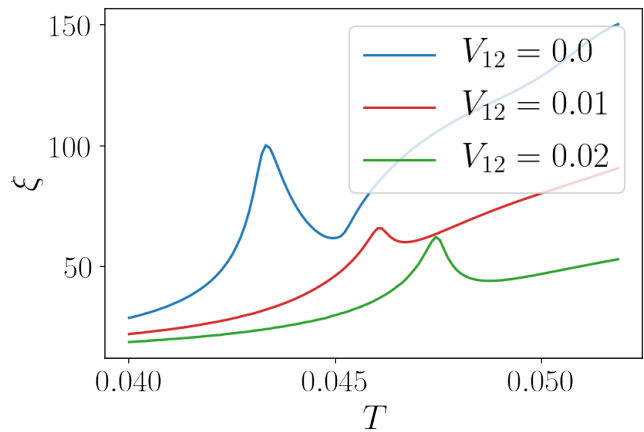


FIG. 4. Decay length scale $\xi(T)$ of the gaps ratio deviation displayed in Figure 3. $\xi(T)$ is plotted as a function of the temperature T and for different values of the interband coupling. The non monotonic behavior as a function of T is clearly visible. We obtain $\xi(T)$ by fitting the tails (i.e. after $N = 50$ sites from the boundary) of the gaps ratio deviation using an exponential function $f(x) \propto e^{-x/\xi}$, for the different values of T and V_{12} . The remaining parameters used in the simulations are $V_{11} = 1.35$, $V_{22} = 1.36$ and $\mu = 0$.

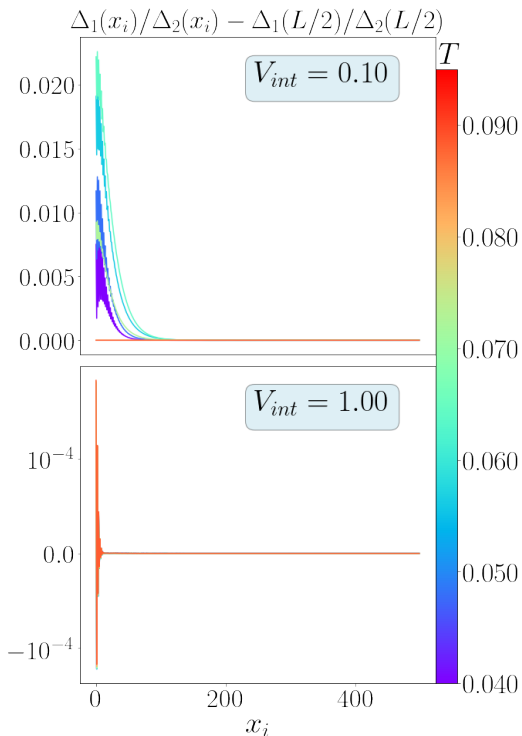


FIG. 5. Suppression of the relative gap variations at stronger interband coupling. We can notice that the gaps ratio change near the boundary is an order of magnitude smaller for $V_{12} = 0.1$ than for $V_{12} = 0.01$. For strong interband coupling $V_{12} = 1$, in the simplest two-band model, the surface-induced change of the gaps ratio is negligible. Also in this case we show only half of the system (500 out of $L = 1000$ sites), since the second half is symmetrical. The parameters used for these calculations are $V_{11} = 1.35$, $V_{22} = 1.36$ and $\mu = 0$.

Next we consider the boundary states when the difference between the intraband potential is greater. Specifically we consider $V_{11} = 1.35$ and $V_{22} = 1.68$. The upper panel of Figure 6 shows the gaps Δ_1 (solid line) and Δ_2 (dashed line) at various temperatures. The bottom panel displays the variation of the gaps ratio with respect to the bulk value. Here the interband potential is set to be $V_{12} = 0.1$. We can see a moderate increase of V_{22} yields a substantial variation of the relative gap values near the surface compared to Figure 5.

Surface effects in two-dimensions and corner states

In 2D and 3D single-component BCS models there are superconducting corner and edge states with relative critical temperature higher than the bulk critical temperature [24, 27]. In this section, we consider the gaps ratio spatial profile in a two dimensional two-band system. In 2D we have edges and corners, therefore we can associate T_{c2} as the mean-field critical temperature for edge superconductivity, and T_{c3} as the mean-field critical tem-

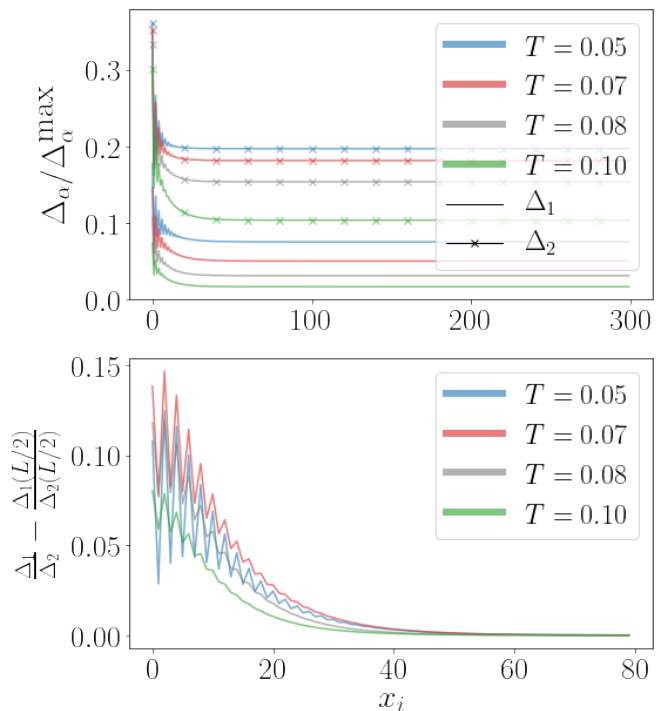


FIG. 6. Numerically obtained order parameters for different values of the T . In this case, we study a coupled two-band system where the difference between the two intraband potentials V_{11} and V_{22} is higher, namely 25%. The upper panel displays the gaps Δ_1 (solid line) and Δ_2 (crossed line) independently. The bottom panel reports the gaps ratio near-surface spatial variation relative to the bulk value. For both panels we fixed $V_{12} = 0.1$. We can notice that the modest increase in V_{22} results in substantially larger variation of the gap ratio near the boundary. Both results were obtained for a system with $N = 1000$ and $\mu = 0$.

perature for corner superconductivity. In a single-band BCS 2D system, $T_{c3} > T_{c2}$, as shown in [27]. We study the two-band system for $T < T_{c1}$, $T_{c1} < T < T_{c2}$ and $T_{c2} < T < T_{c3}$. Studying the boundary effects in two dimensions is challenging, as it requires numerically solving significantly large systems, to avoid the finite-size effects' influence on the resulting states. Figure 7 shows the gaps ratio shifted by its value in the bulk, and the two gaps Δ_1 , Δ_2 . We can notice that the boundary states exist at much smaller length scales than the size of the sample. Both for the bulk ($T = 0.75$) and the edge ($T = 0.77$) states the gaps ratio is enhanced along the system boundaries. When the temperature exceeds the edge critical temperature $T_{c2} = 0.774$, the superconductivity ceases to exist along the boundaries, but remains in the four corners. We observe that in the corners there is the largest variation of the gaps ratio, which decays into the bulk at a macroscopic length scale.

CONCLUSIONS

We investigated the boundary effects in the standard two-band Bardeen-Cooper-Schrieffer theory of superconductivity. We show that, at the level of mean-field theory, the system has multiple critical temperatures, associated to the presence of boundary states. Similarly to the single-band case [24], the effect originates from an increase of the density of states near the boundaries, due to Friedel oscillations. This allows highly inhomogeneous solutions, for the superconducting gap, to survive up to temperatures higher than the standard critical temperature of homogeneous solutions (T_{cl}). We found that the dependence of the critical temperatures on the value of interband coupling is non-monotonic. Moreover, we found that the presence of a boundary state, at weak interband coupling induces a relative variation of the gaps values localized near the boundaries of the system: the ends for the one dimensional case, and the edges and corners for a two dimensional system. The effect is stronger in the sample's corners. The relative variation of the gaps values extends into the superconductor with a large temperature-dependent length scale.

ACKNOWLEDGEMENTS

The work was supported by the Swedish Research Council Grants No. 642-2013-7837, 2016-06122, 2018-03659, the Göran Gustafsson Foundation for Research in Natural Sciences and Medicine, Olle Engkvists Stiftelse.

* alben@kth.se

- [1] H. Suhl, B. T. Matthias, and L. R. Walker, *Phys. Rev. Lett.* **3**, 552 (1959).
- [2] V. Moskalenko, *Fiz. Metal. Metalloved* **8**, 2518 (1959).
- [3] A. Kreisel, P. J. Hirschfeld, and B. M. Andersen, *Symmetry* **12**, 1402 (2020).
- [4] A. Chubukov, *Annu. Rev. Condens. Matter Phys.* **3**, 57 (2012).
- [5] I. Mazin and V. Antropov, *Physica C: Superconductivity* **385**, 49 (2003).
- [6] A. P. Mackenzie, T. Scaffidi, C. W. Hicks, and Y. Maeno, *npj Quantum Materials* **2**, 1 (2017).
- [7] R. Sharma, S. D. Edkins, Z. Wang, A. Kostin, C. Sow, Y. Maeno, A. P. Mackenzie, J. S. Davis, and V. Madhavan, *Proceedings of the National Academy of Sciences* **117**, 5222 (2020).
- [8] J. Böker, P. A. Volkov, K. B. Efetov, and I. Eremin, *Physical Review B* **96**, 014517 (2017).
- [9] S. Zhao, H.-Y. Song, L. Hu, T. Xie, C. Liu, H. Luo, C.-Y. Jiang, X. Zhang, X. Nie, J.-Q. Meng, *et al.*, *Physical Review B* **102**, 144519 (2020).
- [10] G. Rubio-Bollinger, H. Suderow, and S. Vieira, *Phys. Rev. Lett.* **86**, 5582 (2001).
- [11] M. Tsindlekht, G. Leviev, I. Asulin, A. Sharoni, O. Millo, I. Felner, Y. B. Paderno, V. Filippov, and M. Belogolovskii, *Physical Review B* **69**, 212508 (2004).
- [12] M. Belogolovskii, I. Felner, and V. Shaternik, in *Boron Rich Solids* (Springer, 2010) pp. 195–206.
- [13] R. Khasanov, D. Di Castro, M. Belogolovskii, Y. Paderno, V. Filippov, R. Brütsch, and H. Keller, *Physical Review B* **72**, 224509 (2005).
- [14] V. Gasparov, N. Sidorov, and I. Zver'Kova, *Physical Review B* **73**, 094510 (2006).
- [15] P. Biswas, F. Rybakov, R. Singh, S. Mukherjee, N. Parzyk, G. Balakrishnan, M. Lees, C. Dewhurst, E. Babaev, A. Hillier, *et al.*, *Physical Review B* **102**, 144523 (2020).
- [16] H. Fink and W. Joiner, *Physical Review Letters* **23**, 120 (1969).
- [17] R. Lortz, T. Tomita, Y. Wang, A. Junod, J. Schilling, T. Masui, and S. Tajima, *Physica C: Superconductivity* **434**, 194 (2006).
- [18] E. Janod, A. Junod, T. Graf, K.-Q. Wang, G. Triscone, and J. Muller, *Physica C: Superconductivity* **216**, 129 (1993).
- [19] R. A. Butera, *Physical Review B* **37**, 5909 (1988).
- [20] I. Khlyustikov, *Journal of Experimental and Theoretical Physics* **113**, 1032 (2011).
- [21] I. Khlyustikov, *Journal of Experimental and Theoretical Physics* **122**, 328 (2016).
- [22] I. Mangel, I. Kapon, N. Blau, K. Golubkov, N. Gavish, and A. Keren, *Physical Review B* **102**, 024502 (2020).
- [23] V. Ginzburg, *Phys. Letters* **13** (1964).
- [24] A. Samoilenka and E. Babaev, *Physical Review B* **101**, 134512 (2020).
- [25] A. Samoilenka and E. Babaev, “Microscopic derivation of superconductor-insulator boundary conditions for ginzburg-landau theory revisited. enhanced superconductivity with and without magnetic field,” (2020), arXiv:2011.09519 [cond-mat.supr-con].
- [26] E. Bascones and F. Guinea, *Physical Review B* **64**, 214508 (2001).
- [27] A. Samoilenka, M. Barkman, A. Benfenati, and E. Babaev, *Physical Review B* **101**, 054506 (2020).
- [28] A. Weiße, G. Wellein, A. Alvermann, and H. Fehske, *Rev. Mod. Phys.* **78**, 275 (2006).
- [29] L. Covaci, F. M. Peeters, and M. Berciu, *Phys. Rev. Lett.* **105**, 167006 (2010).
- [30] Y. Nagai, Y. Ota, and M. Machida, *Journal of the Physical Society of Japan* **81**, 024710 (2012), <https://doi.org/10.1143/JPSJ.81.024710>.
- [31] M. Silaev and E. Babaev, *Phys. Rev. B* **84**, 094515 (2011).
- [32] M. Silaev and E. Babaev, *Physical Review B* **85**, 134514 (2012).
- [33] J. Carlström, E. Babaev, and M. Speight, *Phys. Rev. B* **83**, 174509 (2011).

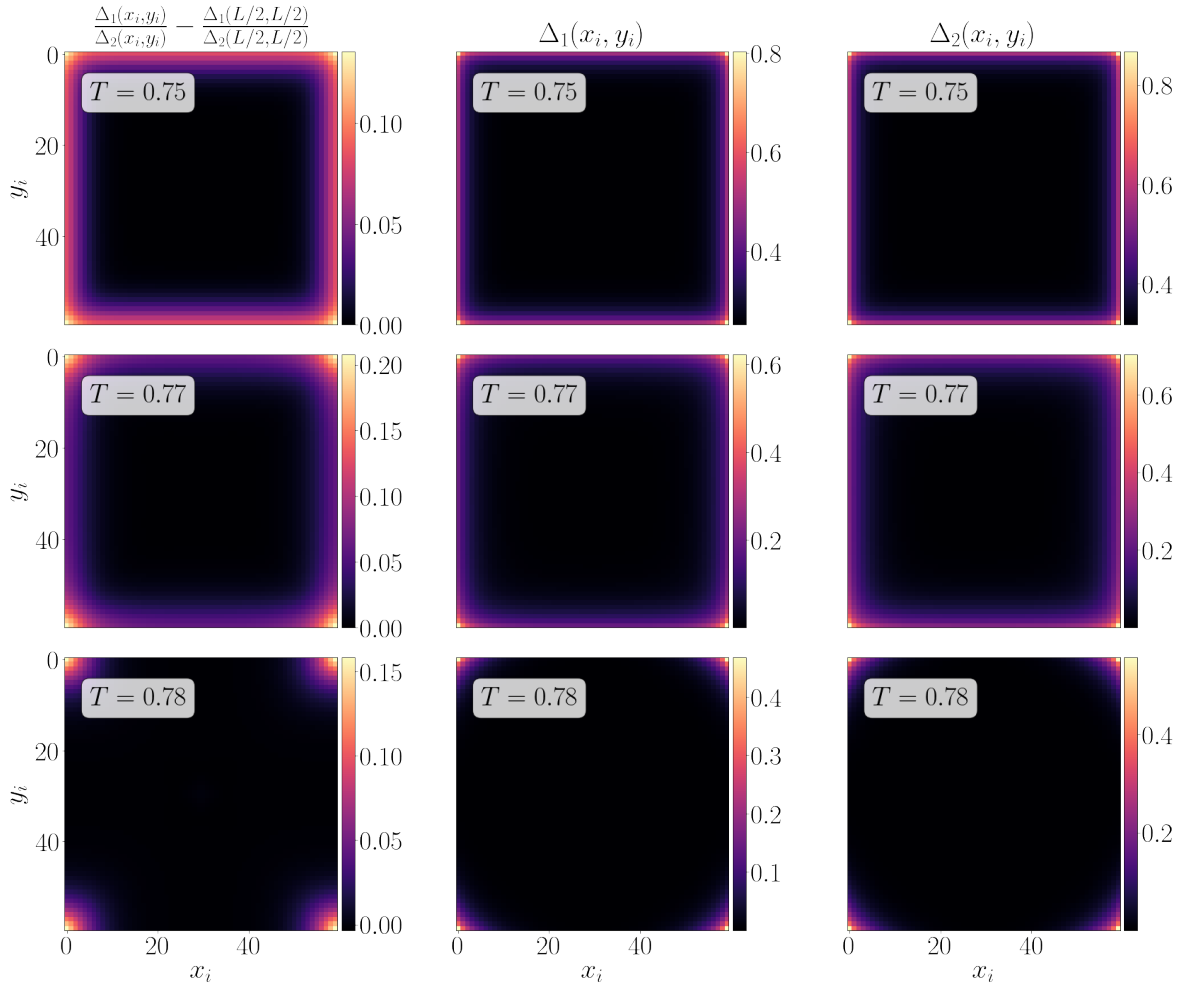


FIG. 7. Plot of the gaps ratio shifted by the bulk value (left column), Δ_1 (center column) and Δ_2 (right column) in two dimensions for increasing temperatures. The bulk critical temperature for the system reads $T_{c1} = 0.759$ and the edge critical temperature is $T_{c2} = 0.774$. Therefore the first row shows the bulk superconductivity, the second row shows the edge superconductivity and the third row shows the state where the gap survives only in the corners. Below the corner critical temperature, i.e. for bulk and edge states we can notice the gradient of the gaps ratio localized along the system's boundaries. The increase is more pronounced above the bulk critical temperature, i.e. with edge states. When $T_{c2} < T < T_{c3}$ superconductivity survives in the four corners, where also the gaps ratio undergoes significant enhancement, penetrating into the bulk with macroscopic length scale.